Journal of Hepatocellular Carcinoma

Dovepress
Taylor & Francis Group

Open Access Full Text Article

ORIGINAL RESEARCH

Low Indoleamine 2,3-Dioxygenase 1 Expression Enhances Dendritic Cells Response to Tumor Cells Against Hepatocellular Carcinoma

Chan Mo[1,2], Min Hong[1], Yunjia Li[1], Danping Huang[1], Qingyu Ji[3], Yuan Liu[3]

[1]Department of First Clinical Medical College, Guangdong Pharmaceutical University, Guangzhou, Guangdong, 510006, People's Republic of China; [2]Medical Laboratory of the Third Affiliated Hospital of Shenzhen University, Shenzhen, Guangdong, 518001, People's Republic of China; [3]College of Integrated Traditional Chinese and Western Medicine, Jining Medical University, Jining, Shandong, 272067, People's Republic of China

Correspondence: Yuan Liu, College of Integrated Traditional Chinese and Western Medicine, Jining Medical University, No. 133, Hehua Road, Taibai Lake New District, Jining City, Shandong Province, 272067, People's Republic of China, Email liuy1015@126.com

Aim: To investigate the effect of IDO1 expression levels in HCC on the distribution, infiltration, and anti-tumor immune response of mature DCs.

Methods: Multiplex immunohistochemical staining was applied to detect the expression level of IDO1 and the infiltration of DCs in the HCC tissue microarray, including total 96 human HCC samples and 82 samples of matched adjacent normal tissues. In vitro, CCK-8, Key Fluor 488 Click-iT Edu, wound healing, and transwell assays were performed to explore the effect of IDO1 on the viability, proliferation, migration and invasion ability of HCC cell line SK-HEP1. In vivo, a subcutaneous xenograft tumor model of nude mice was established by subcutaneously inoculating SK-HEP1 and treated with IDO1 catalytic inhibitor epacadostat (EPA) to observe the effect of IDO1 on tumor growth and immune cells infiltration.

Results: Results of clinical tissue microarrays showed that compared with corresponding paracancerous tissues, the infiltration of mature DCs was significantly reduced in HCC cancer tissues with high expression of IDO1. Meanwhile, IDO1 was highly expressed in HCC cancer tissues with pathological grade I–II, high AFP levels (≥200μg/L), HBV-positivie, cirrhosis, distant metastasis and recurrence. Survival analysis showed that low IDO1 and high mature DCs cell infiltration were significantly associated with superior overall survival (OS). Correlation analysis further showed that IDO1 was negatively correlated with mature DCs. The in vitro cellular and in vivo animal experiments in this study showed that inhibition IDO1 helped to decrease the malignant biological behavior of HCC and enhance the response of immune cells to tumor cells.

Conclusion: IDO1 suppresses anti-tumor immunity in HCC, at least in part, by curtailing mDC infiltration. Targeting IDO1 may represent a promising immunotherapeutic strategy. However, its immunomodulatory effects must be validated in immunocompetent or humanized animal systems before clinical translation.

Keywords: hepatocellular carcinoma, indoleamine 2,3 dioxygenase 1, dendritic cells, T cells

Introduction

Primary liver cancer is a common and serious liver malignant tumor. Globally, its morbidity and mortality rank fifth and fourth, respectively.[1] It is one of the more common and serious diseases in the digestive system. According to the data reported by the National Cancer Center of China, in 2022, the number of new cases of primary liver cancer was 367,700, ranking the fourth among the number of new cases of various cancers and the fifth in the morbidity rate.[2,3] Primary liver cancer mainly includes three different pathological types: hepatocellular carcinoma (HCC), intrahepatic cholangiocarcinoma (ICC), and mixed hepatocellular carcinoma-cholangiocarcinoma (HCC-CC), which are quite different in terms of their pathogenesis, biological behaviours, pathohistology, therapeutic methods, and prognosis. HCC accounts for 75%–85% of the incidence rate of primary liver cancer, and ICC accounts for 10%–15%.[4,5] Risk factors for the development of HCC include various factors such as viral infection, excessive alcohol consumption, aflatoxin, and metabolic-associated

Received: 30 April 2025
Accepted: 16 September 2025
Published: 20 September 2025

Graphical Abstract

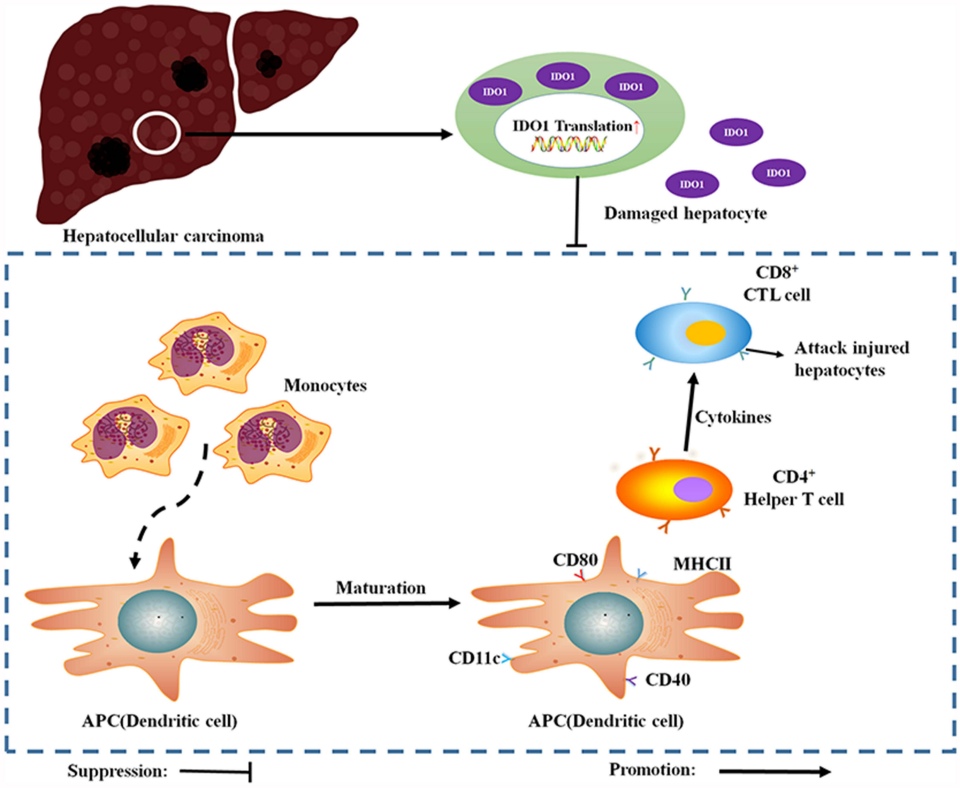

fatty liver disease.[6,7] Although in recent years, people have made rapid progress in the diagnosis and treatment of liver cancer, it has not been able to effectively improve the prognosis of HCC.[8] For early-stage HCC and ICC limited to the liver, treatment is mainly carried out through surgical resection and ablation. However, the recurrence rate within 5 years after treatment can be as high as 40%–70%.[9] Furthermore, approximately 70% of patients are already in an advanced stage of the disease or have complications when diagnosed and cannot undergo radical surgery.[10,11] Recent breakthroughs in immune checkpoint inhibitors (ICIs, e.g, anti-PD-1/PD-L1 antibodies) have revolutionized HCC treatment. However, objective response rates in clinical trials such as KEYNOTE-224 barely exceed 20%, underscoring the urgent need to unravel immunosuppressive mechanisms within the tumor microenvironment (TME).[12,13]

The human indoleamine 2,3-dioxygenase-1 (IDO1) gene is located on chromosome 8, has 10 exons, and is about 15 kb in length; the human IDO1 protein is composed of 403 amino acids with a relative molecular mass of about 45,000, and consists mainly of two α-helices and their encapsulated ferrous haemoglobin moieties.[14] It has been reported that IDO1 can be abnormally highly expressed in a variety of tumor tissues, including gastric cancer,[15] esophageal cancer,[16] pancreatic cancer,[17] breast cancer,[18] and lung cancer.[19] IDO1 was highly expressed in these solid tumors and was associated with immune escape and poor prognosis. Jiao et al revealed that IDO1 expression was upregulated in patients with esophageal squamous cell cancer and predicted poor response and prognosis.[20] Yin et al reported that high IDO1 expression in lung adenocarcinoma correlated with increased tumor invasiveness, metastatic potential, advanced clinical stage, and poorer prognosis.[21] Hu et al reported that overexpression of IDO1 and lower $CD8^+$ T-cell levels were associated with poor survival in patients with gastric cancer and overexpression of IDO1 was associated with the poor tumor response.[22] Shi et al revealed that in colorectal cancer, patients with a low immunoscore or high IDO1 protein levels were significantly associated with poor survival. IDO1 depletes tryptophan (Trp) in the tumor microenvironment by catalyzing Trp metabolism, activates GCN2 kinase, leads to the phosphorylation of eIF2α, and thereby inhibits the proliferation and activation of effector T cells,

inducing T cell incompetence. Meanwhile, the produced kynurenine (Kyn) can activate AhR, promote the differentiation and proliferation of regulatory T cells (Treg), and enhance immunosuppression.[23] The expression of IDO1 in tumor cells could indirectly promote tumor angiogenesis and the formation of hypoxic environments by influencing immune cells and cytokine networks in the tumor microenvironment.[24] Yang Q et al reported IDO1-mediated AhR activation up-regulated pentose phosphate pathway via NRF2 to inhibit ferroptosis in lung cancer.[25] Chow LP et al found that IDO1-induced AhR and β-catenin modulated the expression of proliferation and EMT-related genes to facilitate growth and metastasis of HCC.[26] However, the biological role of IDO1 in HCC has not been fully defined. Some scholars have indicated that increased IDO1 expression in HCC tissues was associated with tumor progression,[27] while other evidence suggested that IDO1 might play an anti-tumor role through regulation of specific immune cell subsets. This paradox implies that the function of IDO1 may be tissue microenvironment-dependent, and the specific regulatory mechanisms of IDO1 on HCC immune escape need to be further elucidated.

IDO is a heme enzyme that catalyzes the oxidative degradation of L-tryptophan (L-Trp) through the kynurenine pathway (KP), generating metabolites that regulate immune responses. These byproducts, mainly kynurenines, contribute to immunosuppression and influence immune cell differentiation, promoting Tregs and inducing apoptosis in inflammatory cells.[28] It was reported that IDO1 could induce macrophage M1 polarization via ER stress-associated GRP78-XBP1 pathway to promote ulcerative colitis progression.[29] And IDO1 could promote $CD8^+$T cell exhaustion by reducing Trp levels in glioblastoma.[30] Kyn, produced by the metabolism of IDO1, is a ligand of AhR. Kyn binds to AhR, induces the expression of FoxP3 in $CD4^+$T cells and blocks the orphan receptor C associated with retinoic acid receptor, differentiates $CD4^+$T cells intoTreg cells and prevents the development of Th17 cells, thereby inducing immune tolerance.[31] Besides, IDO1 could affect the maturation and function of DCs by altering the cytokine profile secreted by DCs, reducing the secretion of IL-12 and increasing the secretion of IL-10. Subsequently, it regulates the activation and proliferation of T cells and the immune response.[32] Many studies have confirmed IDO1 could inhibit the antigen-presenting ability of DCs and macrophages, which in turn inhibit T-cell activation; whereas in NK cells, IDO1 could significantly increase the killing effect of NK cells on tumor cells and promote the anti-tumor immune response.[30,33–35] Yang KD et al reported that increasing NK cell infiltration into tumors could help to improve the efficacy of HCC treatments.[36] DCs are specialized antigen-presenting cells, which play an important role in activating naïve T cells and initiating adaptive immune responses, and are an important bridge between innate and adaptive immunity. As the most potent APCs in the body, DCs upregulate the expression of costimulatory molecules such as CD80, CD86, CD40, and the chemokine receptor upon stimulation with tumor antigens. Zeng et al reported that DCs were stimulated by nasopharyngeal carcinoma antigens and underwent maturation, which might facilitate the activation of cytotoxic T cells and enhance the anti-tumor immune response.[37] DCs could take up tumour antigens and then migrate towards lymph nodes, where they cross-present them to $CD8^+$ T cells, resulting in priming of tumour antigen-specific CTLs.[38] Although DC-based vaccines have shown preclinical efficacy, their clinical translation remains hindered by persistent TME suppression, highlighting the imperative to target upstream immunosuppressive nodes such as IDO1.[39] The dose–response relationship between IDO1 expression level and DCs antitumor activity, especially the dynamic regulatory network in HCC, has not been systematically studied.

Based on the above background, this study focuses on the reprogramming effect of IDO1 expression level on DCs function and its effect on anti-tumor immune response in HCC. By integrating clinical sample analysis, in vitro experiments, and tumor-bearing mice models, we demonstrated that low IDO1 expression in liver cancer tissues could reshape the immunosuppressor state of TME by up-regulating the infiltration of mature DCs and downstream T cells, thereby inhibiting HCC progression. This finding not only provides a new theoretical explanation for the double-edged sword role of IDO1 in HCC but also provides an experimental basis for combining the precision treatment strategy of IDO1 inhibitors with existing immunotherapies (such as PD-1 blocking), which has important translational medicine value.

Materials and Methods

Cell Culture and Treatment

Human-derived hepatocellular carcinoma cell line (SK-HEP1) was purchased from Wuhan Servicebio Technology Co., Ltd (Hubei, China) and has been authenticated by STR profiling. SK-HEP1 cells were cultured in SK-HEP1 cell-specific

culture medium, including 89% MEM basic medium+10% fetal bovine serum+1% penicillin streptomycin mixture (Servicebio, China) in humidiffed cell incubator at 37°C with 5% CO_2. IDO1 catalytic inhibitor epacadostat (EPA) was purchased from MedChemExpress LLC (Shanghai, China). Cells were seeded in 6-well plates or 96-well plates and randomly divided into control and EPA treatment groups with EPA at final concentrations of 2.5, 5, 10 and 20 μM in light of the test data proposed in reference.[40–42]According to different experimental purposes, cells were collected for fixation or extraction of RNA and proteins for subsequent assays after incubation for an appropriate period of time.

Tumor Models and Treatments

All animal experiments were performed in compliance with protocols approved by the Laboratory Animal Ethics Committee of Shenzhen Zhongxun Precision Medicine Research Institute and adhered to the relevant ethical regulations for animal research (Approval number: ZXJZ202306100001). Mice were managed in accordance with the Institutional Animal Care and Use Committee (IACUC) guideline. Male BALB/c nude mice, 4–6 weeks old, were purchased from Guangdong Pharmalab Biotechnology Co., Ltd (Guangdong, China) and kept under specific pathogen-free conditions. Drawing on previous literature reports, we constructed a HCC-bearing mouse model and subsequently performed EPA intervention to investigate its potential effects.[43,44] SK-HEP1 cells (4×10^6 cells/100 μL) in logarithmic growth phase were injected into the right dorsal side of nude mice. Tumor size was measured every 3 days until the end of the experiment, and the tumor volume was calculated according to the formula $V = (a \times b^2)/2$, where a is the largest superficial diameter and b is the smallest diameter. When the tumor volume reached approximately 90 mm^3, mice were randomly distributed to control and experimental group (five mice in each group), and treatment was initiated. Experimental group (EPA-treated) received intraperitoneal injection of EPA (100 mg/kg), every 3 days for a total of 3 injections. EPA solutions were prepared using a solvent containing 5% DMSO + 40% PEG300 + 5% Tween-80 + 50% Saline according to the reagent instructions. Control group was treated with equal dose of solvent without EPA. At the end of the experiment, mice were anesthetized by intraperitoneal injection of 200mg/kg pentobarbital. The blood and fresh tumor tissues were collected and processed for further detection.

Key Fluor 488 Click-iT Edu Assay

Effects of EPA on the proliferation of SK-HEP1 cells were detected using the Key Fluor 488 Click-iT Edu kit (RiboBio, China) according to the product instructions. SK-HEP1 cells in the logarithmic growth phase were inoculated into 96-well plates at a cell density of 1×10^5 per well and adhered overnight. EPA was formulated at working concentrations of 0, 2.5, 5, 10, and 20μM. Three duplicate wells were set for each group, and the intervention lasted for 24 h. Diluted 10mM of the Edu working solution with the medium to 10 μM. Added 100μL of the preheated Edu working solution to each well and incubate for 2 h to label Edu. Discarded the culture medium in the wells and added 4% paraformaldehyde. Fixed at room temperature for 20 min. Discarded the stationary solution, added 50 μL of 2mg/mL glycine solution to each well to neutralize the remaining stationary solution, and incubated at room temperature for 5 mins. Added 100μL of 3% BSA in PBS washing solution to each well and washed the cells twice. After the washing was completed, 100μL of 0.5% Triton X-100 in PBS was added to each well and permeated at room temperature for 20 mins. After washing, added 100 μL of the freshly prepared Click-iT reaction mixture to each well and incubated at room temperature in the dark for 30 mins. After washing, added 100μL 1× Hoechst 33342 working solution to each well and incubated at room temperature in the dark for 10 min. Removed the Hoechst33342 reaction solution. Added 100μL of PBS buffer washing solution to each well to wash the cells twice, then observed and photographed under a fluorescence microscope.

CCK-8 Assay

SK-HEP1 cells in the logarithmic growth phase were inoculated into 96-well plates at a cell density of 1×10^5 per well and adhered overnight. EPA was formulated at working concentrations of 0, 2.5, 5, 10, and 20μM. Three duplicate wells were set for each group, and the intervention lasted for 24 h. CCK-8 kit (Bioswamp, China) was used to detect the effect of EPA on the viability of SK-HEP1 cells. After culturing in the medium containing different concentrations of EPA for 24h, 10 μL of CCK-8 solution was added to the cells, and incubated for 4 h at 37°C. The absorbance of each group of cells was detected at 450 nm using a multifunctional microplate detector (TECAN Spark, Switzerland). The cell viability was calculated in each group according to the instructions.

Wound Healing Assay

Total 7×10^5 SK-HEP1 cells were seeded in a 6-well plate. When the cells reached 85% density, a 10 μL sterile pipette tip was used to draw a straight line vertically on the cell layer. The cells were washed twice with PBS to remove the scratched cell debris. Then, fresh complete medium containing different concentrations of EPA was added for culture. The 6-well plates were observed under a microscope and photographed at 0, 24 h and 48 h, respectively.

Transwell Assay

SK-HEP1 cell suspension was prepared by using FBS-free medium, and the cell density was adjusted to 1×10^6 cells/mL. Two hundred microliter of cell suspension was taken from each group and placed on the upper chamber of Transwell insert (Membrane pore size is 8 μm, Corning, USA), 600 uL of complete medium containing 10% FBS was put into the lower surface of each group. After being cultured in a constant temperature incubator for 24 h, the medium was aspirated from the lower surface of the chamber, and the cells were washed three times with PBS, and the lower surface of each group was fixed with 4% paraformaldehyde for 30 min, 0.1% crystal violet (Beyotime Biotechnology, China) staining for 30 min. The cells on the upper chamber surface were wiped off. Under the microscope, six fields of view were randomly selected from each group to observe and count the cells.

Enzyme Linked Immunosorbent Assay (ELISA)

ELISA was used to detect the Trp and Kyn contents in the serum of tumor-bearing mice after EPA intervention. Each analyte was assessed using a specific ELISA kit, all procured from COIBO BIO, following the manufacturer's detailed instructions. Before the experiment, mouse serum was placed at room temperature for equilibration for 60 mins. Meanwhile, the corresponding ELISA kits were removed from the refrigerated environment and equilibrated at room temperature for 30 mins. Standard wells and sample wells were set up on the microplate. The number of standard wells was determined based on experimental requirements. Fifty microliter of standard substances with different concentrations were added to each standard substance well, respectively. Fifty microliter of the mouse serum sample to be tested was added to the sample well, and no liquid was added to the blank well. Except for the blank wells, 100μL of horseradish peroxidase (HRP)-labeled detection antibody was added to each well of the standard wells and sample wells. The reaction wells were sealed with a sealing film, and the microplate was incubated in a 37°C water bath for 60 mins. After incubation, the liquid in the wells was discarded, and the microplate was turned upside down onto absorbent paper to be patted dry. After washing, 50 μL of Substrate A and 50 μL of Substrate B were added to each well, and the microplate was gently shaken to ensure thorough mixing of the substrates with the liquid in the wells. The microplate was then incubated in a light-proof environment at 37°C for 15 mins. After incubation, 50 μL of stop solution was added to each well, and the microplate was gently shaken to ensure thorough mixing of the liquid. The OD value of each well was measured at a wavelength of 450 nm using a microplate reader (TECAN Spark, Switzerland). The linear regression equation of the standard curve was calculated based on the concentration and corresponding OD value of the standard substance. The OD value of the sample was substituted into the equation to obtain the calculated concentration, which was then multiplied by the dilution factor to determine the actual concentration of the sample.

RNA Extraction, cDNA Synthesis, and qPCR

Total RNA was extracted from the cells according to the instructions of the RNA Extraction Kit (Fastagen, China), and then cDNA was synthesized by reverse transcription of total RNA in accordance with the instructions of the HiScript III RT SuperMix for qPCR (Vazyme, China). qPCR was performed with RealStar Green Fast Mixture (GenStar, China) in Applied Biosystems QuantStudio Dx system. GAPDH was used as endogenous control. Three duplicate holes were set for each group. After the PCR reaction was completed, first determined whether the primers were appropriate based on the amplification curve, dissolution curve and CT value of PCR. Then, obtained the relative expression level of the target gene mRNA through the CT value of the target gene and the CT value of the internal reference gene detected simultaneously on the machine. The results were normalized against the GAPDH gene and expressed as relative target abundance using the 2-ΔΔCt method. Sequence-specific primers for the genes detected are listed as following:

GAPDH (human)-F, 5′-AGAAGGCTGGGGCTCATTTG-3′,
GAPDH (human)-R, 5′-GCAGGAGGCATTGCTGATGAT-3′;
E-cadherin (human)-F, 5′-ATTTTTCCCTCGACACCCGAT-3′,
E-cadherin (human)-R, 5′-TCCCAGGCGTAGACCAAGA-3′;
Vimentin (human)-F, 5′-AGTCCACTGAGTACCGGAGAC-3′,
Vimentin (human)-R, 5′-CATTTCACGCATCTGGCGTTC-3′;
IDO1 (human)-F, 5′- GCCTGATCTCATAGAGTCTGGC-3′,
IDO1 (human)-R, 5′-TGCATCCCAGAACTAGACGTGC −3′;
PCNA (human)-F, 5′- AGAGGAGGAAGCTGTTACCATAGAG-3′,
PCNA (human)-R, 5′-CATACTGAGTGTCACCGTTGAAGAG-3′.

Western Blot Analysis

Total cellular protein was extracted and quantified according to the instructions of Total Protein Extraction Lysate (Beyotime Biotechnology, China) and BCA protein assay kit (EpiZyme, China). Then, total proteins were separated by 10% SDS-PAGE (EpiZyme, China) and then transferred onto a PVDF membrane (Millipore, USA). After membrane transfer, the membrane was blocked for 10 min with NcmBlot blocking buffer (NCM Biotech, China). After washing with TBST, incubated the primary antibody overnight at 4°C, including IDO1 (clone D5J4E, 1:1000, rabbit, CST), E-cadherin (clone 24E10, 1:1000, rabbit, CST), Vimentin (clone D21H3, 1:1000, rabbit, CST), GAPDH (1:3000, rabbit, proteintech) and α-tubulin (1:3000, rabbit, proteintech), followed by incubation with HRP-conjugated secondary antibodies (1:5000, rabbit, proteintech). After imaging by chemiluminescence, Quantity One was used to analyze the gray value of the image and calculate the relative expression level of protein.

Multiplex Immunohistochemistry Analysis

We performed multiple immunohistochemical staining according to the instructions for the Opal 7-color Manual IHC Kit (PerkinElmer, USA). The tissue microarray (HLivH180Su31) employed in this study, including total 96 human HCC samples and 82 samples of matched adjacent normal tissues, was purchased from Shanghai Outdo Biotech Co. Ltd (Shanghai, China). Before the research began, they had already obtained the corresponding ethical approval. The use of these tissue samples all conformed to ethical standards and obtained the informed consent of the patients. The specific ethics approval number was SHYJS-CP-2206007, which was approved by the Ethics Committee of Shanghai Superchip Biotechnology Co., LTD. All patients' personal information was strictly confidential and used only for scientific research purposes. Tissue microarrays were routinely deparaffinized and antigenically repaired. After blocking, primary antibodies and horseradish peroxidase (HRP)-conjugated secondary antibodies were used for staining sequentially and stained with one of the seven Opal reagents, followed by microwave intervention to remove the primary and secondary antibodies before another round of staining. Anti-IDO1 (clone D5J4E, 1:250, rabbit, CST), anti-CD11C (1:200, rabbit, Proteintech), anti-CD80 (clone RM1133, 1:200, rabbit, Abcam), anti-CD40 (clone EPR20735, 1:100, rabbit, Abcam), anti-MHCII (clone SC06-78, 1:150, rabbit, HUABIO) and anti-keratin (1:200, rabbit, Proteintech) were used as primary antibodies. The dyes Opal520, Opal650, Opal480, Opal690, Opal570, Opal620 and DAPI were used for staining. Samples were visualized and analyzed using the Tissue Gnostics (TissueFAXS SpectraS, Peking, China).

Histopathology, Immunofluorescence and Immunohistochemical Staining

For histopathological staining, tumor tissues were fixed with 4% paraformaldehyde for 24 h, routinely dehydrated in gradient, embedded in paraffin sections, cut into 4 μm-thick sections. HE staining were conducted according to the reagent instructions (Servicebio, China).

For immunohistochemical staining, we performed routine baking, dewaxing to water for paraffin sections of tumor tissues, antigen repair, blocking endogenous peroxidase. Then, the slices were incubated with PCNA antibody (rabbit, proteintech) at 4°C overnight in a wet box. The subsequent steps was carried out according to the instructions of the immunochromatography kit (Servicebio, China). The slides were scanned under the Digital Pathology Slice Scanner (KFBIO, China).

For immunofluorescence staining, before staining, performed routine dewaxing and rehydration, microwave antigen heat repair, and blocking. Next, primary antibodies were added and samples were incubated overnight at 4°C. After washing with PBS three times, added the corresponding secondary antibodies, incubated at room temperature in the dark for 50 min, followed by staining the nuclei with DAPI (Solarbio Life Science, China) then observed under the fluorescence microscope (Nikon Eclipse Ti-SR, Japan). The following primary antibodies were used: anti-IDO1 (clone 1G1, 1:100, rabbit, HUABIO), anti-CD11C (1:250, rabbit, Servicebio), anti-CD80 (clone 1E2F10, 1:200, mouse, Proteintech), anti-CD40 (clone PSH10-01, 1:100, rabbit, HUABIO), anti-MHCII (clone SC06-78, 1:100, rabbit, HUABIO), anti-CD4 (1:200, rabbit, Servicebio) and anti-CD8 (1:400, mouse, Servicebio).

Statistical Analyses

All data were presented as means ± SEM. Statistical analyses were performed through SPSS22 (IBM Corp, USA) and GraphPad Prism 9 (GraphPad Software, USA). Data were compared using independent-samples *t*-test for two groups or one-way ANOVA for multi-group variable comparisons. Statistically significant differences were considered at $*P < 0.05$, $**P < 0.01$ and $***P < 0.001$. The prognostic significances of IDO1 expression and mature DCs infiltration were evaluated using the Kaplan–Meier method and were compared with the log-rank test. A Cox regression model was used to perform univariate analyses, and multivariate analysis was performed on all factors with $P < 0.05$. Overall survival was defined as the length of time from the surgery date to death or until the last follow-up (censored). The correlations among the expression levels of IDO1 and mature DCs were analyzed using Spearman's rank correlation.

Results

IDO1 Expression Was Related to Poor Prognosis in HCC

To evaluate the possible significance of IDO1 in the development of HCC, we used immunofluorescence staining to detect IDO1 expression level in HCC tissue microarray. The valid sample size in results was smaller than the total stated in methods, due to technical issues (detachment, staining failure, or weak signals) during microarray staining/scanning. Of 96 cancer tissues, 23 were excluded, leaving 73 for statistical analysis. We found that the fluorescence intensity of IDO1 in HCC tissues were significantly increased compared with that in paracancerous tissues (Figure 1A). We divided the samples into the IDO1-low expression group and the IDO1-high expression group based on the median fluorescence density of IDO1. Survival analysis has shown favorable OS were highlighted by Kaplan–Meier curves for HCC patients with low-IDO1 expression compared with those with high-IDO1expression (Figure 1B). To define the potential functional role of IDO1 to the outcome of HCC, we further studied the association of IDO1 expression with clinicopathologic and prognostic features in HCC. Results showed that there was no significant association between IDO1 expression and age (Figure 1C), gender (Figure 1D), tumor size (Figure 1E), HBcAb (Figure 1L). IDO1 expression was lower in HCC tissues with pathologic grade III–IV compared to those with pathologic grade I–II (Figure 1F). Moreover, HCC tissues from patients with high AFP levels (≥200ug/L), HBV-positive, cirrhosis, metastasis, and relapse presented higher expression levels of IDO1 compared with those from patients with low AFP levels (<200ug/L), HBV-negative and the absence of cirrhosis, metastasis, and relapse (Figure 1G–K). These findings indicated that IDO1 was highly expressed in HCC tissues and related to poor prognosis.

The Infiltration and Prognostic Significance of Mature DCs Subsets in HCC

It is known that the tumor immune microenvironment is closely related to the occurrence and development of tumors. Our previous research has shown that IDO1 could be used as a key biological target for hepatic fibrosis, the early pathological process of HCC. By mediating the Trp metabolic pathway, IDO1 could inhibit the maturation of the immune phenotype of DCs, affect the immune microenvironment in the liver, and participate in regulating the process of hepatic fibrosis.[45] To comprehensively characterize the infiltration of mature DCs, we conducted m-IHC analysis to evaluate the infiltration of mature DCs. In this paper, DCs were identified as the $CD11C^+$, and mature DCs were identified as the $CD11C^+CD80^+$, $CD11C^+CD86^+$, $CD11C^+CD40^+$, $CD11C^+MHCII^+$, according to references literatures.[46–48]

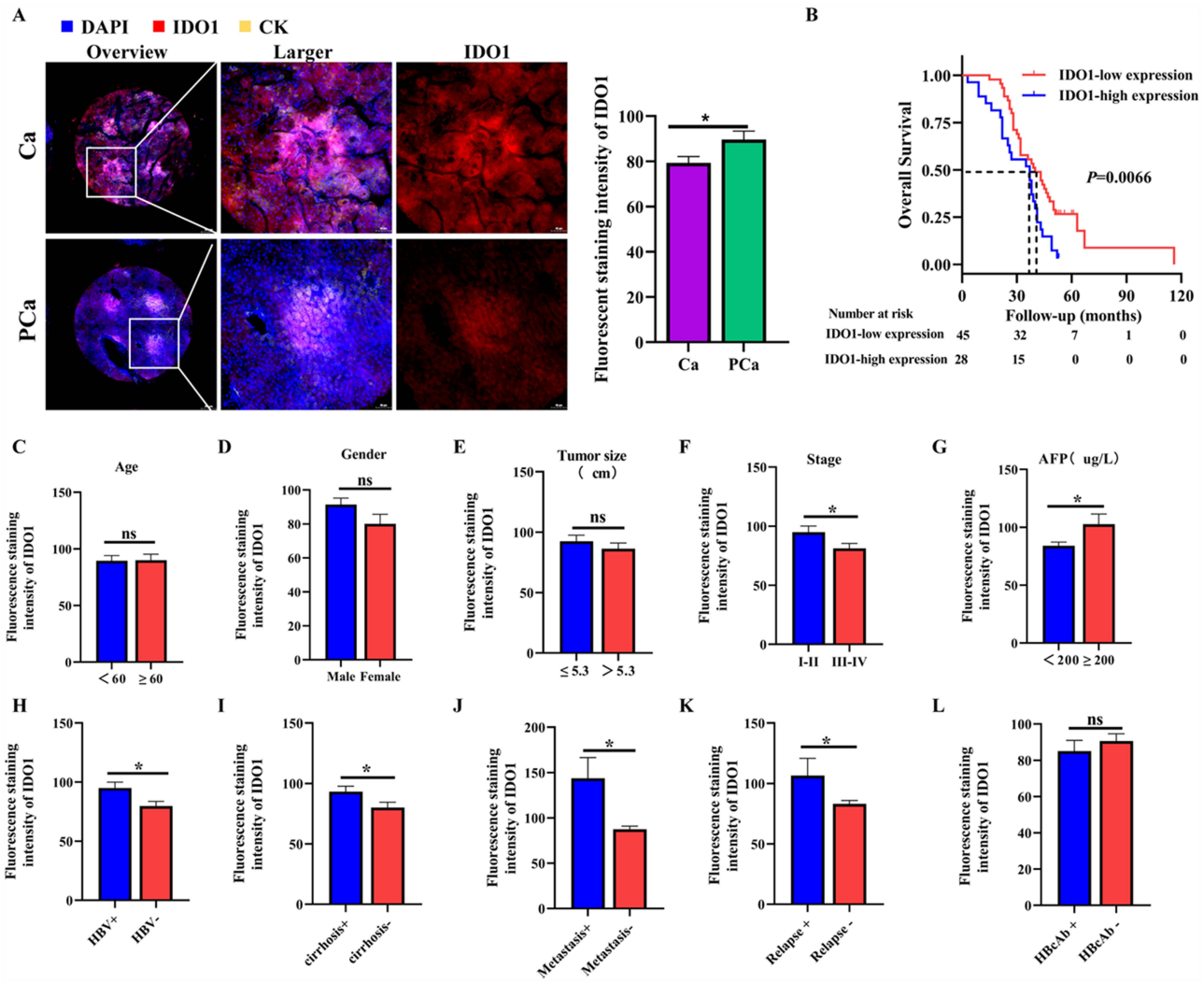

Figure 1 IDO1 expression was related to poor prognosis in HCC. (**A**) Representative images of IDO1 immunofluorescence staining of HCC tissue and paracancerous tissue in patients with HCC and quantitative results of the fluorescence intensity of IDO1. (**B**) Kaplan–Meier curves for OS in HCC patients based on IDO1expression level. (**C**) The IDO1 expression grouped by age, gender (**D**), tumor size (**E**), stage (**F**), AFP (**G**), HBV (**H**), cirrhosis (**I**), metastasis (**J**), relapse (**K**) and HBcAb (**L**). The data were presented as mean ± SEM (*P< 0.05).

Abbreviations: Ca, Cancer; Pca, Paracancerous; DAPI, 4′,6-Diamidino-2-phenylindole; CK, Cytokeratin; IDO1, Indoleamine 2,3 dioxygenase 1; AFP, Alpha-Fetoprotein; HBV, Hepatitis B Virus; HBcAb, Hepatitis B core antibody.

Representative m-IHC staining images were shown in Figure 2A. In the HCC tissues, the percentage of $CD11C^+$, $CD11C^+MHCII^+$, $CD11C^+CD80^+$ and $CD11C^+CD40^+$DCs were significantly lower than those of the corresponding paracancerous tissues (Figure 2B). To investigate the survival difference of the infiltration of mature DCs in HCC, overall survival rates were analyzed by Kaplan–Meier survival curves. As shown in Figure 2C–F, HCC patients with the high infiltration of $CD11C^+$, $CD11C^+MHCII^+$, $CD11C^+CD80^+$ and $CD11C^+CD40^+$DCs had significantly more favourable OS than those with low infiltration of $CD11C^+$, $CD11C^+MHCII^+$, $CD11C^+CD80^+$ and $CD11C^+CD40^+$DCs. Moreover, Spearman correlation analysis revealed the negative correlation between the infiltration of $IDO1^+$ cells and the infiltration of $CD11C^+MHCII^+$, $CD11C^+CD80^+$ and $CD11C^+CD40^+$DCs in HCC (Figure 2G–I). Together, these results suggest that IDOl might be responsible for establishing the immune tolerance mechanism of HCC and affect the prognosis of patients with HCC.

Analysis of Risk Factors Affecting OS in Patients with HCC

In order to understand the correlation between various clinicopathological parameters, the expression level of IDO1 and the overall survival (OS) rate of HCC patients, we conducted univariate and multivariate Cox proportional hazards model

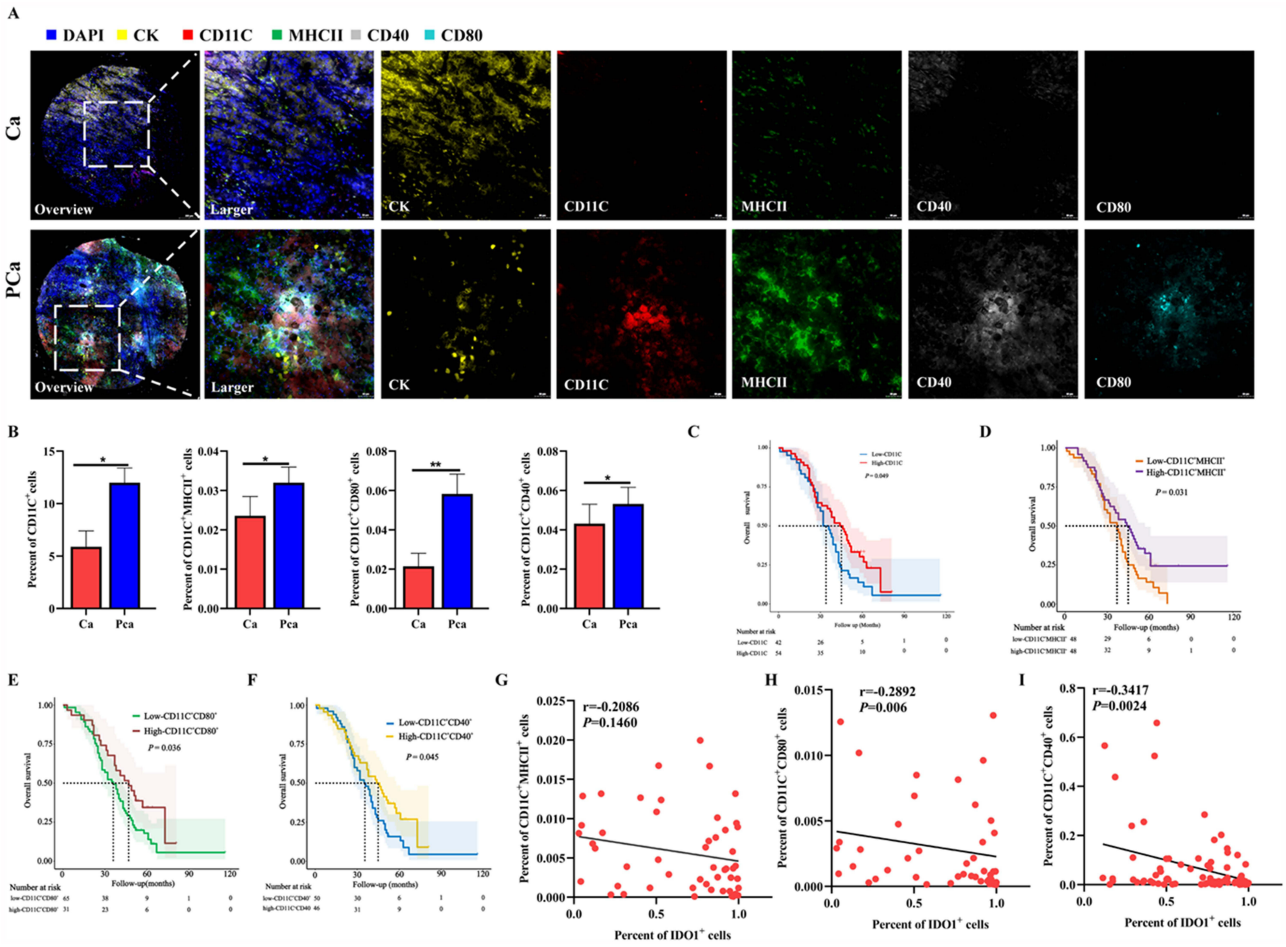

Figure 2 The infiltration and prognostic significance of mature DCs subsets in HCC. (**A**) Representative images of immunofluorescence staining of CK, CD11C, MHCII, CD40, CD80, in cancer and paracancerous tissues from HCC patients. (**B**) Quantitative analysis of the percentage of $CD11C^+$, $CD11C^+MHCII^+$, $CD11C^+CD80^+$ and $CD11C^+CD40^+$ DCs. (**C**) Kaplan–Meier curves for OS in HCC patients based on the percentage of $CD11C^+$DCs. (**D**) Kaplan–Meier curves for OS in HCC patients based on the percentage of $CD11C^+MHCII^+$DCs. (**E**) Kaplan–Meier curves for OS in HCC patients based on the percentage of $CD11C^+CD80^+$DCs. (**F**) Kaplan–Meier curves for OS in HCC patients based on the percentage of $CD11C^+CD40^+$DCs. (**G**) The correlation between the percentage of $IDO1^+$ staining area levels and the percentage of $CD11C^+MHCII^+$DCs, according to Spearman correlation analysis. (**H**) The correlation between the percentage of $IDO1^+$ staining area levels and the percentage of $CD11C^+CD80^+$DCs, according to Spearman correlation analysis. (**I**) The correlation between the percentage of $IDO1^+$ staining area levels and the percentage of $CD11C^+CD40^+$DCs, according to Spearman correlation analysis. The data were presented as mean ± SEM (*P< 0.05, **P<0.01).

Abbreviations: Ca, Cancer; Pca, Paracancerous; DAPI, 4′,6-Diamidino-2-phenylindole; CK, Cytokeratin; IDO1, Indoleamine 2,3 dioxygenase 1; CD11C, Cluster of Differentiation 11C; MHCII, Major Histocompatibility Complex Class II; CD40, Cluster of Differentiation 40; CD80, Cluster of Differentiation 80.

analyses on these factors for OS in patients with HCC. Univariate Cox regression proportional risk model analysis revealed that $CD11C^+MHCII^+$DCs, $CD11C^+CD80^+$ DCs, $CD11C^+CD40^+$ DCs and HBcAb were protective factors affecting the prognosis of HCC patients. Age and distant metastasis were risk factors for poor prognosis in patients with HCC. Multifactorial Cox regression proportional risk model analysis confirmed that age and distant metastasis were independent risk factors for poor prognosis in HCC patients (Table 1).

IDO1 Inhibition Could Attenuate the EMT and Malignant Proliferation of SK-HEP1 in vitro

To explore the influence of IDO1 on the malignant biological behaviors of HCC, we inhibited IDO1 in SK-HEP1 cells with EPA and observed the biological changes in vitro. As shown in Figure 3A, 20 μM, 5μM, 2.5 μM EPA could decrease IDOl protein expression level in SK-HEP1 cells significantly. Q-PCR analysis showed substantially decreased IDO1 mRNA level in 20 μM EPA-treated group than in control group (Figure 3C). Results of Western blot showed that IDO1 inhibition caused an increase in the expression of the epithelial marker E-cadherin and a decrease in mesenchymal

 https://doi.org/10.2147/JHC.S530997

Table 1 Univariate and Multivariate Analysis Results of Cox Regression Proportional Risk Model for OS in HCC Patients

Variables	Univariate Analysis			Multivariate Analysis		
	HR	95% CI	*P* Value	HR	95% CI	*P* Value
IDO1$^+$Mean Intensity	1.003	0.726–1.803	0.398	/	/	/
CD11C$^+$MHCII$^+$cells(%)	0.61	0.39–0.96	0.0306	0.79	0.47–1.34	0.383
CD11C$^+$CD80$^+$cells(%)	0.60	0.36–0.98	0.0404	0.67	0.32–1.39	0.283
CD11C$^+$CD40$^+$cells(%)	0.64	0.41–0.10	0.048	1.17	0.58–2.34	0.661
Sex	0.80	0.42–1.51	0.486	/	/	/
Age	2.07	1.30–3.30	0.00204	2.11	1.28–3.48	0.00358
Tumor_size	1.09	0.70–1.70	0.698	/	/	/
T	1.49	0.93–2.39	0.0966	/	/	/
N	7.41	0.96–56.95	0.0544	/	/	/
M	26.84	5.29–136.10	0.0000715	26.04	4.58–147.98	0.000235
Grade	2.23	1.40–3.57	0.000818	1.43	0.82–2.48	0.209
TNM	1.49	0.93–2.39	0.0966	/	/	/
Distal_metastases	26.84	5.29–136.11	0.0000715	26.04	4.58–147.98	0.000235
Lymph.node_metastasis	7.41	0.96–56.95	0.0544	/	/	/
Cirrhosis	1.08	0.68–1.71	0.757	/	/	/
HBsAg	1.37	0.86–2.16	0.184	/	/	/
HBcAb	0.50	0.28–0.87	0.0138	0.55	0.3–1.03	0.0606
HCVAb	0.94	0.23–3.86	0.934	/	/	/
AFP (ug/L)	1.41	0.91–2.20	0.126	/	/	/

marker Vimentin as compared with control cells (Figure 3A and B). We also determined that the RNA level of E-cadherin in EPA-treated SK-HEP1 cells were remarkably increased and Vimentin was decreased as compared with control cells (Figure 3C). Additionally, proliferating cell nuclear antigen (PCNA) plays a crucial role in the initiation of cell proliferation and is an excellent indicator of the proliferative state of cells. Higher levels of PCNA expression in tumor cells indicate greater proliferative activity and higher degrees of malignancy.[49] As expected, both PCNA protein and RNA expression level were down-regulated in EPA-treated SK-HEP1 cells as compared with control cells (Figure 3B and C). In summary, these results indicated that IDO1 inhibition could alleviate the degree of EMT and malignant proliferation of SK-HEP1 cells.

IDO1 Inhibition Could Reduce the Viability, Proliferation, Invasion and Migration of SK-HEP1 Cells in vitro

To investigate the potential role of IDO1 in the development of HCC, CCK-8, Edu, transwell and wound healing assays were performed to assess IDO1 inhibition on the viability, proliferation, invasion and migration of SK-HEP1 cells in vitro. Edu assay revealed that treatment with 20 μM and 10μM EPA could reduce the proliferation level of SK-HEP1 cells dramatically (Figure 4A and B). Consistently, CCK-8 assays also revealed that 20 μM, 10μM and 5μM EPA could significantly reduce the viability of SK-HEP1 cells (Figure 4C). Furthermore, through transwell and wound-healing assays, we found that, the invasion and migration ability of SK-HEP1 cells in the 20 μM and 10μM EPA-treated group were significantly reduced compared with that in the control group (Figure 4D and E). These results suggest that the decreased malignant biological behavior of SK-HEP1 cells observed were likely attributed to the inhibition of IDO1.

IDO1 Inhibition Could Delay the Subcutaneous Tumor Formation of SK-HEP1 Cells in vivo

Given that IDO1 inhibition could attenuate the malignant biological behavior of SK-HEP1 in vitro, we further established a xenograft tumor model by inoculating SK-HEP1 cells subcutaneously on the right back of nude mice to explore the

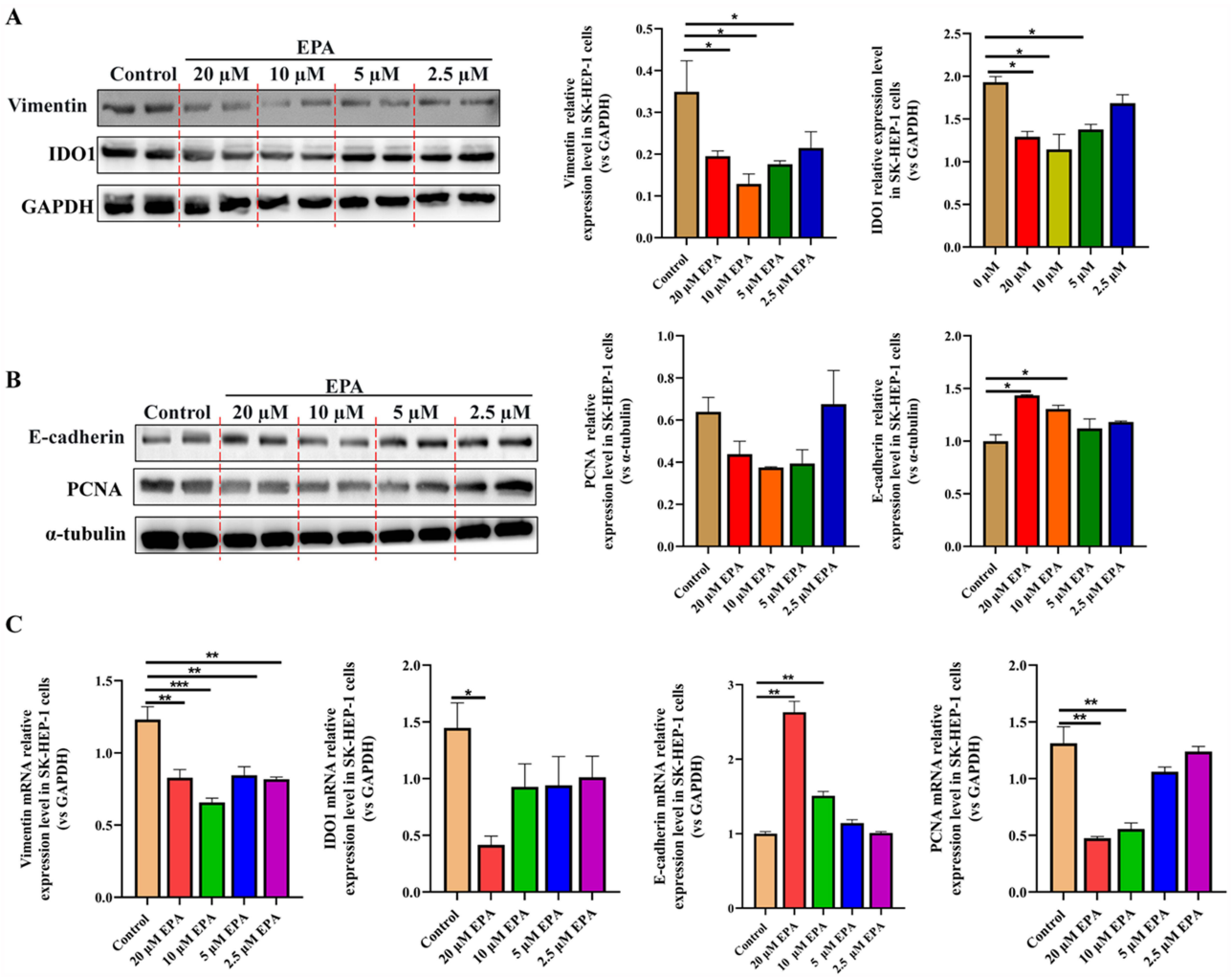

Figure 3 IDO1 inhibition could attenuate the EMT and malignant proliferation of SK-HEP1 in vitro. (**A**) Western blot analysis was used to detect the expression levels of Vimentin and IDO1 in control and experimental SK-HEP1 cells at 24 h after EPA intervention. GAPDH served as a loading control. The density of protein was measured using Quantity One software. (**B**) Western blot analysis was used to detect the expression levels of E-cadherin and PCNA in control and experimental SK-HEP1 cells at 24 h after EPA intervention. α-tubulin served as a loading control. The density of protein was measured using Quantity One software. (**C**) Relative mRNA levels of IDO1, E-cadherin, Vimentin, and PCNA were measured in SK-HEP1 cells treated with 0, 2.5, 5, 10, and 20 μM EPA for 24 h. The data were presented as mean ± SEM (*P< 0.05, **P<0.01, ***P< 0.001).

Abbreviations: IDO1, Indoleamine 2,3 dioxygenase 1; GAPDH, Glyceraldehyde-3-Phosphate Dehydrogenase; PCNA, Proliferating Cell Nuclear Antigen; EPA, Epacadostat.

effect of IDO1 on HCC cell growth in vivo. The experimental procedure is shown in Figure 5A. As reflected in Figure 5D and E, compared with the control group, the protein expression level of IDO1 was reduced in the tumor tissues of the experimental group significantly intervened with EPA. We further detected the Trp and Kyn contents in the serum of tumor-bearing mice after EPA intervention. Consistent with existing reports, compared with the control group, the serum levels of Trp in tumor-bearing mice after EPA intervention were significantly increased, and the levels of Kyn were significantly decreased, indicating that EPA indeed inhibited the activity of IDO1 in catalyzing the metabolism of Trp to Kyn. According to the tumor growth curves in Figure 5B and C, both the volume and weight of the tumors in the EPA-treated group of tumor-bearing mice were significantly reduced compared with control group. HE staining of tumor tissues in the two groups revealed that in the control group, the tumor cells were in good growth status, abundant and tightly arranged between cells, with unequal cell sizes and deeply stained nuclei, and there were obvious necrotic foci, which was in line with the morphologic characteristics of tumor cells. In the EPA-treated group, the number of tumor cells were significantly reduced, the length and diameter of the tumor was significantly shorter than that of the control group, and the arrangement between cells was loose (Figure 5F). We have previously found that both PCNA protein and

https://doi.org/10.2147/JHC.S530997

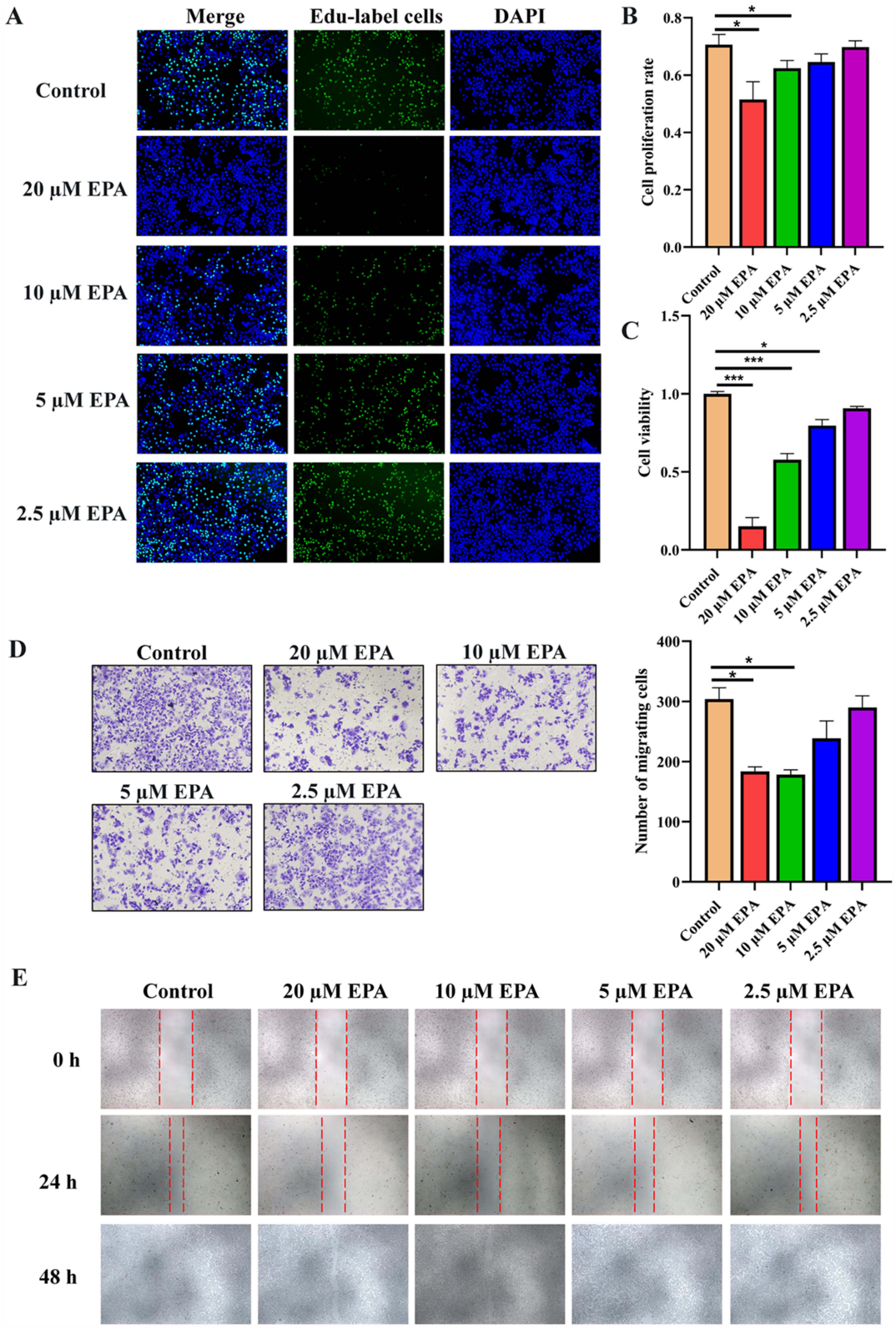

Figure 4 IDO1 inhibition could improve the malignant biological behavior of SK-HEP1 cells in vitro. (**A**) The proliferation of SK-HEP1 cells treated with 0, 2.5, 5, 10, and 20 μM EPA for 24 h was evaluated using the Key Fluor 488 Click-iT Edu assay. (**B**) The proliferation rate of SK-HEP1cells in (**A**) was quantified in a bar graph. (**C**) The cell viability of SK-HEP1 cells treated with 0, 2.5, 5, 10, and 20 μM EPA for 24 h was assessed using the CCK-8 assay. The cell viability reported as fold change of EPA-treated vs control cells. (**D**) Representative images from the transwell assay (left) and migrating cells number analysis (right). (**E**) Representative images from the wound healing assay. The data were presented as mean ± SEM (*P< 0.05, ***P< 0.001).

Abbreviations: DAPI, 4′,6-Diamidino-2-phenylindole; EPA, Epacadostat; Edu, 5-Ethynyl-2′-deoxyuridine.

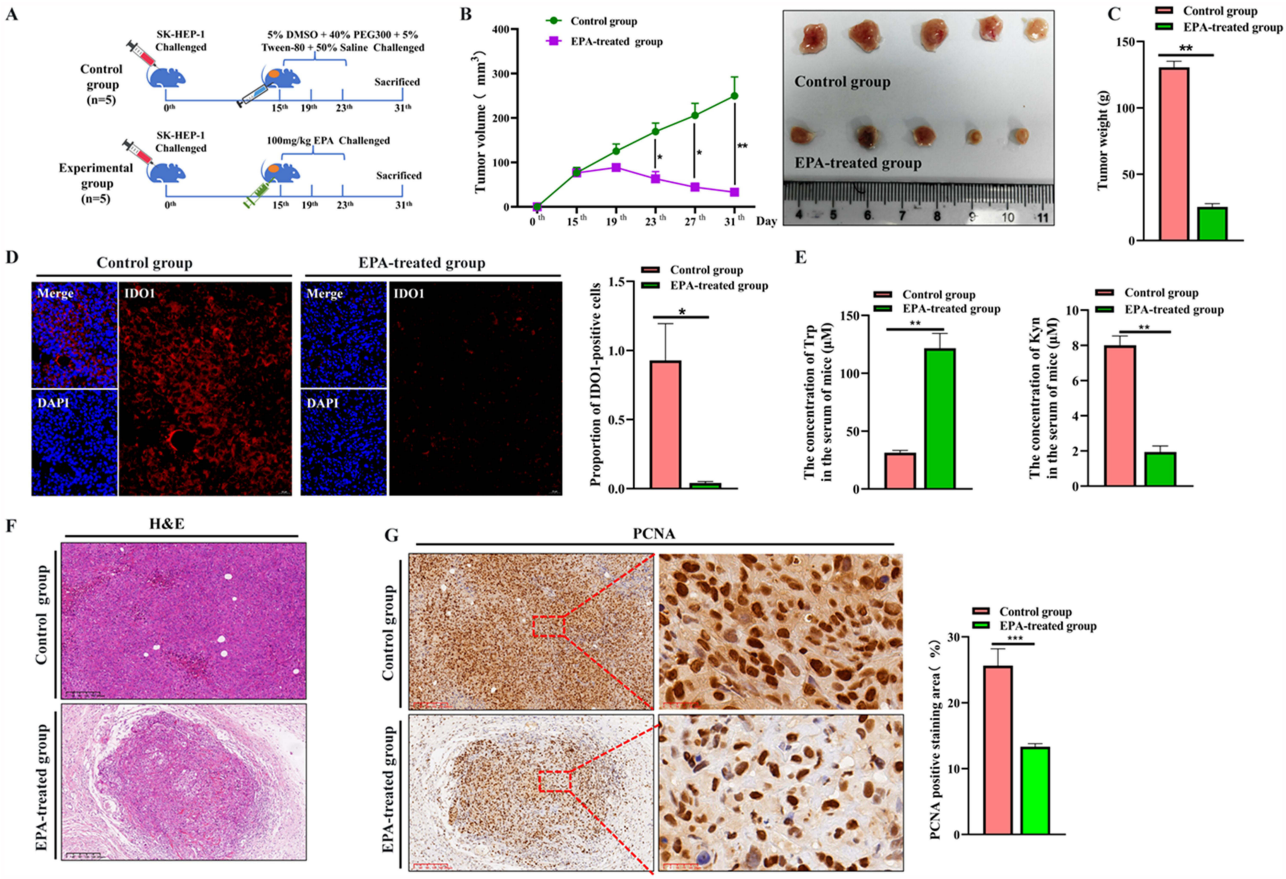

Figure 5 IDO1 inhibition could delay the subcutaneous tumor formation of SK-HEP-1 cells in vivo. (**A**) Schematic protocol for animal experiment. (**B**) The tumor growth curve of mice and the representative diagrams of tumors in each group. (**C**) Tumor weight of the mice in control and EPA-treated group. (**D**) Immunofluorescence staining of IDO1 in tumor tissues in control and EPA-treated group. (**E**) The serum levels of Trp and Kyn were determined in mice from both the control and EPA-treated groups. (**F**) HE staining of tumor tissues in control and EPA-treated group. (**G**) Immunohistochemistry staining of PCNA in control and EPA-treated group. The data were presented as mean ± SEM (*P< 0.05, **P<0.01, ***P< 0.001).

Abbreviations: DAPI, 4′,6-Diamidino-2-phenylindole; EPA, Epacadostat; IDO1, Indoleamine 2,3 dioxygenase 1; H&E, Hematoxylin and Eosin; PCNA, Proliferating Cell Nuclear Antigen.

RNA expression level decreased in EPA-treated SK-HEP1 cells in vitro. The protein expression level of PCNA in tumors was further analyzed by immunohistochemical staining. We detected a significant decrease on the expression intensity of PCNA in the tumor tissues from the EPA-treated group compared to those from controls (Figure 5F). Taken together, these data indicated that, IDO1 inhibition could significantly reduce the growth rate of SK-HEP1 cells in vivo and delay SK-HEP1 xenograft tumor growth.

IDO1 Inhibition Could Enhance Immune Cells Response to Tumor Cells in vivo

As outlined above, IDO1 expression was correlated with the infiltration of mature DCs in HCC patients. Additionally, we investigated the infiltration of mature DCs in HCC tissues from tumor-bearing mice following IDO1 inhibition. Immunofluorescence staining verified that an increased proportion of infiltrated $CD11C^+$, $MHCII^+$, $CD80^+$, $CD40^+$DCs cells, and $CD4^+$, $CD8^+$T cells were observed in tumor tissues after administrating EPA (Figure 6A and B), indicated that IDO1might involved in the regulation of DCs and T cells response to tumor cells.

Discussion

By integrating clinical HCC samples, in vitro cell experiments and animal models, this study revealed the inhibitory effect of IDO1 on the infiltration of mature DCs and anti-tumor immune response in the HCC microenvironment, and provided evidence for its use as a potential therapeutic target. Our core findings suggest that HCC tissues with IDO1 high

https://doi.org/10.2147/JHC.S530997

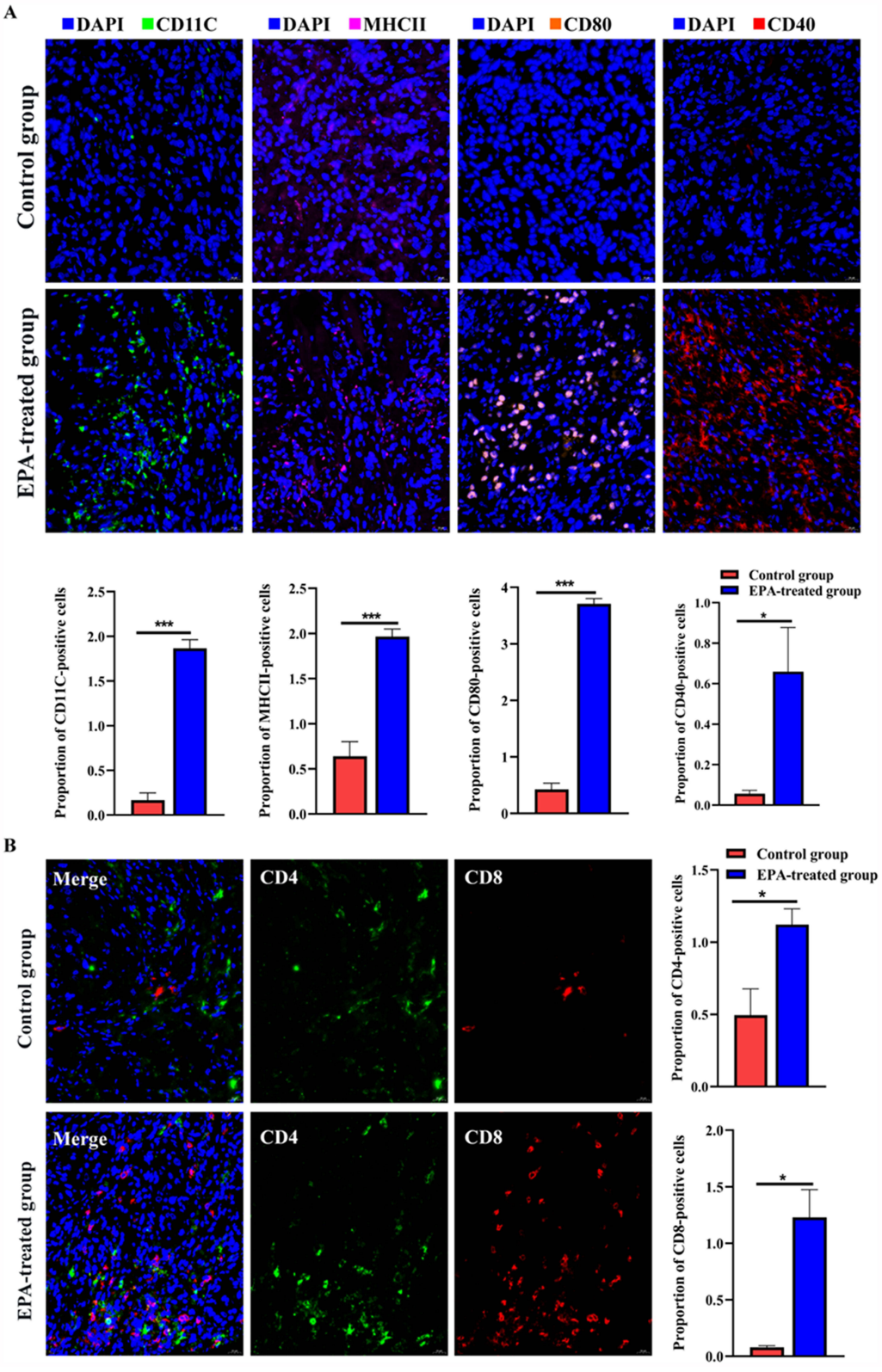

Figure 6 IDO1 inhibition could enhance immune cells response to tumor cells in vivo. (**A**) Immunofluorescence staining of CD11C, MHCII,CD80 and CD40 in tumor tissues in control and EPA-treated group. (**B**) Immunofluorescence staining of CD4 and CD8 in tumor tissues in control and EPA-treated group. The data were presented as mean ± SEM (*P< 0.05, ***P< 0.001).

Abbreviations: DAPI, 4′,6-Diamidino-2-phenylindole; CD11C, Cluster of Differentiation 11C; MHCII, Major Histocompatibility Complex Class II; CD40, Cluster of Differentiation 40; CD80, Cluster of Differentiation 80; CD4, Cluster of Differentiation 4; CD8, Cluster of Differentiation 8.

expression show significantly reduced infiltration of mature DCs and were strongly associated with aggressive clinical features (including, high AFP, HBV positive, metastasis/recurrence) and poor prognosis. Notably, IDO1 expression levels were inversely correlated with the proportion of infiltrated mature DCs in HCC. This finding complements the mechanism reported in previous studies, wherein IDO1 promotes Treg differentiation via the Kyn-AHR pathway,[50] may contribute to the establishment of a pathological axis of "IDO1 high expression →DCs function depletion → immune escape" in HCC.

Published literatures indicated that IDO1 could induce phenotypic changes of DCs through various mechanisms in the tumor microenvironment, thus promoting immune tolerance and tumor immune escape. IDO1 catalyzes the metabolism of Trp to produce Kyn and its downstream metabolites that activate the AhR signaling pathway. Activation of AhR inhibits DCs maturation, reduces the expression of co-stimulatory molecules (eg, CD80, CD86, MHCII) on the surface of DCs, and decreases their ability to activate T cells, thereby inducing immune tolerance.[51,52] Accelerated Trp metabolism leads to local Trp depletion and activation of the GCN2 kinase signaling pathway, which can also inhibit DCs maturation and function in mice with intracerebral hemorrhage.[53] The expression of IDO1 in DCs can also confer an immune tolerance phenotype that is independent of its enzyme activity. ITIM (immune receptor tyrosine inhibitory motif) in the IDO1 molecule recruits SHP-1/SHP-2 phosphatase, which in turn inhibits immune activation signaling in DCs.[54] In celiac disease patients, DCs with high expression of IDO1 can amplify Tregs cells, which further inhibit DCs maturation by secreting immunosuppressive cytokines such as TGF-β and IL-10.[55] Here, we found that the percentage of $CD11C^{+}MHCII^{+}$, $CD11C^{+}CD80^{+}$ and $CD11C^{+}CD40^{+}$DCs were significantly reduced in HCC tissues with high expression of IDO1. And an increased proportion of infiltrated $CD11C^{+}$, $MHCII^{+}$, $CD80^{+}$, $CD40^{+}$DCs cells, and $CD4^{+}$, $CD8^{+}$T cells were observed in tumor tissues after inhibiting IDO1.

In clinical application, this study provided an important basis for the targeted therapy of IDO1 in HCC. IDO1 was highly expressed in HCC tissues with pathological grade I–II, high AFP levels (≥200ug/L), HBV-positivie, cirrhosis, distant metastasis and recurrence, suggested that these patients might be the priority beneficiary group of IDO1 catalytic inhibitors. The expression level of IDO1 by Western blot as well as q-PCR, confirmed that EPA treatments led to decreased levels of IDO1 in SK-HEP1 cells. It was reported that EPA (firstly named INCB024360) was one of the most promising catalytic inhibitors targeting IDO1 to foster anti-tumor immune responses.[56] Many studies[57–62] have confirmed that the intervention of EPA could reduce the expression level of IDO1, which were consistent with the results of this study. In animal models, EPA treatment significantly reduced tumor volume, accompanied by increased DCs and T cell infiltration, suggesting that inhibition of IDO1 could potentially reverse the immunosuppressive microenvironment of HCC.

Survival analysis showed that low IDO1 and high mature DCs cell infiltration were significantly associated with superior OS. These findings may support the use of IDO1 expression in combination with DCs infiltration distribution as a biomarker to guide therapeutic stratification in HCC. However, it is important to note the potential limitations of the clinical application of IDO1 catalytic inhibitors. The limited efficacy of single-agent EPAs in solid tumors in clinical trials might be related to their failure to synchronize the blockade of other pathways depleted of DCs (eg, PD-L1/PD-1).[63] DC vaccine, as a new method of cancer immunotherapy, has made remarkable progress in clinical research in recent years, showing great application potential.[64] Bol KF et al announced the Phase III clinical data of DC vaccine treatment in stage IIIB/C melanoma patients, which generated specific immune responses and was well tolerated with a 2-year survival rate of over 80%.[65] Recently, van Eijck CHJ et al published a study on the efficacy of SOC therapy and DC-based adjuvant immunotherapy in preventing recurrence of pancreatic cancer in patients with pancreatic cancer, which showed that the 2-year RFS rate after pancreatectomy was 64%, suggesting that DC-based immunotherapy can significantly prevent recurrence of pancreatic cancer.[66] It is worth noting that the results of the current clinical trials of IDO1 catalytic inhibitors and also DC vaccines are not all helpful in improving the prognosis of cancer patients, probably due to patient selection, combination therapy and other factors, and better treatment options need to be further investigated. For HCC, taking into account the findings of the present study, we can next explore the synergistic treatment options of IDO1 catalytic inhibitors in combination with PD-1 blockade or DCs vaccine or enhancement of DCs response based on the stratification of patients with IDO1 expression levels, so as to improve the efficacy of targeted therapies.

This study, through comprehensive experimental design and multi-faceted analysis, revealed the mechanism of IDO1 in HCC, especially its inhibitory effect on the infiltration of mature DCs and the anti-tumor immune response. It not only

enriches the understanding of the immune microenvironment of HCC but also provides new ideas and strategies for the diagnosis, prognosis assessment and immunotherapy of HCC. Meanwhile, there are some limitations in this study. The clinical sample size was small and the functional association of IDO1 expression levels with DCs subpopulations was not analyzed. The in vitro experiments only used SK-HEP1 cell line, which needs to be expanded to HCC cell lines of different molecular subtypes. Animal models using immunodeficient mice failed to fully mimic the regulatory effects of IDO1 on the adaptive immune system. Nude mice exhibit thymic deficiency, resulting in incomplete T-cell development and consequent immune system impairments. This characteristic can reduce the interference of the normal immune system on tumors, providing convenience for the study of biological behaviors such as tumor growth and metastasis. However, it also poses a challenge to the interpretation of immune cell infiltration results. Although nude mice are typically regarded as lacking functional T cells, accumulating evidence indicates that small populations of cells expressing T-cell markers (eg, Thy-1) can be detected in these animals. The numbers of such cells tend to increase with age or under specific pathological conditions (eg, hepatitis).[67–70] Moreover, functional $CD4^+$ and $CD8^+$ T cells, as well as IL-2-secreting T cells, have been identified in the tumor tissues of nude mice in several studies.[71–78] Consistent with these reported immune cell characteristics of nude mouse models, our study detected DCs and a small number of infiltrating T cells in tumor tissues via immunohistochemistry. To address the limitations of the nude mouse model, we further validated the potential impact of low IDO1 expression on immune cell infiltration trends through correlation analyses between IDO1 and DC markers using clinical liver cancer tissue microarrays. Nevertheless, it is important to emphasize that as nude mice lack a fully functional adaptive immune system, while they can be used to study certain aspects of the immune microenvironment, there are limitations in drawing comprehensive conclusions about immune cell infiltration, especially regarding T cell-mediated adaptive immune responses. Consequently, the immune-infiltration findings should be regarded as hypothesis-generating rather than definitive. Robust validation in immunocompetent syngeneic models, humanized mouse systems, or patient-derived organoid-immune cell co-cultures is indispensable before clinical translation. These results nonetheless provide valuable preliminary insights for exploring the role of IDO1 in the tumor immune microenvironment.

Conclusions

In summary, this study delineates a dual, clinically relevant role for IDO1 in HCC immune evasion, directly fostering tumor aggressiveness while concurrently suppressing anti-tumor immunity, notably by curbing mature DCs infiltration. These findings provide a theoretical framework for precision immunotherapies centered on IDO1 inhibition. Nevertheless, because our *in-vivo* experiments were performed in nude mice that lack a functional adaptive immune system, the immune-infiltration data must be interpreted cautiously. Follow-up work should therefore (I) validate the immunomodulatory effects of IDO1 blockade in immunocompetent or humanized mouse models, (II) dissect the molecular crosstalk between IDO1 and additional immune checkpoints, and (III) optimize combination regimens tailored to the HCC-specific immune microenvironment.

Data Sharing Statement

The datasets used and/or analysed during the current study are available from the corresponding author on reasonable request.

Ethics Approval Statement

All animal experiments were conducted in accordance with the protocols approved by the Laboratory Animal Ethics Committee of Shenzhen Zhongxun Precision Medicine Research Institute and compliance with the relevant ethical regulations for animal research (Approval number:ZXJZ202306100001). Mice were managed in accordance with the Institutional Animal Care and Use Committee (IACUC) guideline.

Acknowledgments

This paper has been uploaded to ResearchSquare as a preprint: https://www.researchsquare.com/article/rs-5300369/v1.

Author Contributions

All authors reviewed the manuscript. All authors made a significant contribution to the work reported, whether that is in the conception, study design, execution, acquisition of data, analysis and interpretation, or in all these areas; took part in drafting, revising or critically reviewing the article; gave final approval of the version to be published; have agreed on the journal to which the article has been submitted; and agree to be accountable for all aspects of the work.

Funding

This work was supported by the Natural Science Foundation of Guangdong Province (2021A1515110861, 2025A1515010076), National Natural Science Foundation of China (82204841) and Shenzhen Medical Research Fund (A2303020).

Disclosure

The authors declare that they have no competing interests in this work.

References

1. Rumgay H, Arnold M, Ferlay J. et al. Global burden of primary liver cancer in 2020 and predictions to 2040. *J Hepatol*. 2022;77(6):1598–1606. doi:10.1016/j.jhep.2022.08.021
2. Han B, Zheng R, Zeng H, et al. Cancer incidence and mortality in China, 2022. *J Natl Cancer Cent*. 2024;4(1):47–53. doi:10.1016/j.jncc.2024.01.006
3. Zheng R, Zhang S, Zeng H, et al. Cancer incidence and mortality in China, 2016. *J Natl Cancer Cent*. 2022;2(1):1–9. doi:10.1016/j.jncc.2022.02.002
4. Bray F, Ferlay J, Soerjomataram I, et al. Global cancer statistics 2018: GLOBOCAN estimates of incidence and mortality worldwide for 36 cancers in 185 countries. *CA Cancer J Clin*. 2018;68(6):394–424. doi:10.3322/caac.21492
5. Li X, Ramadori P, Pfister D, et al. The immunological and metabolic landscape in primary and metastatic liver cancer. *Nat Rev Cancer*. 2021;21(9):541–557. doi:10.1038/s41568-021-00383-9
6. Hao L, Li S, Deng J, et al. The current status and future of PD-L1 in liver cancer. *Front Immunol*. 2023;14:1323581. doi:10.3389/fimmu.2023.1323581
7. Chan YT, Zhang C, Wu J, et al. Biomarkers for diagnosis and therapeutic options in hepatocellular carcinoma. *Mol Cancer*. 2024;23(1):189. doi:10.1186/s12943-024-02101-z
8. Li M, Tang Y, Wang D, et al. Sphingosine-1-phosphate transporter spinster homolog 2 is essential for iron-regulated metastasis of hepatocellular carcinoma. *Mol Ther*. 2022;30(2):703–713. doi:10.1016/j.ymthe.2021.09.012
9. Zhou J, Sun H, Wang Z, et al. Guidelines for the Diagnosis and Treatment of Hepatocellular Carcinoma (2019 Edition). *Liver Cancer*. 2020;9(6):682–720. doi:10.1159/000509424
10. Xiang Y, Wu J, Qin H. Advances in hepatocellular carcinoma drug resistance models. *Front Med*. 2024;11:1437226. doi:10.3389/fmed.2024.1437226
11. Zhou J, Sun H, Wang Z, et al. Guidelines for the Diagnosis and Treatment of Primary Liver Cancer (2022 Edition). *Liver Cancer*. 2023;12(5):405–444. doi:10.1159/000530495
12. Finn RS, Qin S, Ikeda M, et al. Atezolizumab plus Bevacizumab in Unresectable Hepatocellular Carcinoma. *N Engl J Med*. 2020;382(20):1894–1905. doi:10.1056/NEJMoa1915745
13. Wu J, Liu W, Qiu X, et al. A Noninvasive Approach to Evaluate Tumor Immune Microenvironment and Predict Outcomes in Hepatocellular Carcinoma. *Phenomics*. 2023;3(6):549–564. doi:10.1007/s43657-023-00136-8
14. Fujiwara Y, Kato S, Nesline MK, et al. Indoleamine 2,3-dioxygenase (IDO) inhibitors and cancer immunotherapy. *Cancer Treat Rev*. 2022;110:102461. doi:10.1016/j.ctrv.2022.102461
15. Wang Y, Jin Y, Wang T, et al. IDO1 as a potential diagnostic biomarker for gastric cancer. *Asian J Surg*. 2024;47(10):4351–4353. doi:10.1016/j.asjsur.2024.06.072
16. Yao W, Cui X, Peng H, et al. IDO1 facilitates esophageal carcinoma progression by driving the direct binding of NF-κB and CXCL10. *Cell Death Discov*. 2023;9(1):403. doi:10.1038/s41420-023-01689-3
17. Liang H, Zhan J, Chen Y, et al. Tryptophan deficiency induced by indoleamine 2,3-dioxygenase 1 results in glucose transporter 1-dependent promotion of aerobic glycolysis in pancreatic cancer. *MedComm*. 2024;5(5):e555. doi:10.1002/mco2.555
18. Zhuo X, Deng H, Qiu M, et al. Pathomic model based on histopathological features and machine learning to predict IDO1 status and its association with breast cancer prognosis. *Breast Cancer Res Treat*. 2024;207(1):151–165. doi:10.1007/s10549-024-07350-6
19. Bessede A, Peyraud F, Le Moulec S, et al. Upregulation of Indoleamine 2,3-Dioxygenase 1 in Tumor Cells and Tertiary Lymphoid Structures is a Hallmark of Inflamed Non-Small Cell Lung Cancer. *Clin Cancer Res*. 2023;29(23):4883–4893. doi:10.1158/1078-0432.CCR-23-1928
20. Jiao R, Zheng X, Sun Y, et al. IDO1 Expression Increased After Neoadjuvant Therapy Predicts Poor Pathologic Response and Prognosis in Esophageal Squamous Cell Carcinoma. *Front Oncol*. 2020;10:1099. doi:10.3389/fonc.2020.01099
21. Yin Z, Sun B, Wang S, et al. Investigating the role of IDO1 in tumors: correlating IDO1 expression with clinical pathological features and prognosis in lung adenocarcinoma patients. *PeerJ*. 2025;13:e18776.
22. Chen H, Zheng Q, Jiang Y, et al. IDO1 Expression and CD8+ T-Cell Levels Are Useful Prognostic Biomarkers in Preoperative Gastric Cancer Specimens Before Neoadjuvant Chemotherapy. *Appl Immunohistochem Mol Morphol*. 2025;33(1):1–9. doi:10.1097/PAI.0000000000001238

23. Pallotta MT, Rossini S, Suvieri C, et al. Indoleamine 2,3-dioxygenase 1 (IDO1): an up-to-date overview of an eclectic immunoregulatory enzyme. *FEBS J*. 2022;289(20):6099–6118. doi:10.1111/febs.16086
24. Shen SC, Dey S, DuHadaway JB, et al. Neovascular pruning by IDO1 inhibitors can potentiate immunogenic cytotoxicity of ischemia-targeted agents to synergistically enhance anti-PD-1 responsiveness. *J Immunother Cancer*. 2025;13(5):e011398. doi:10.1136/jitc-2024-011398
25. Zhan J, Chen Y, Liu Y, et al. IDO1-mediated AhR activation up-regulates pentose phosphate pathway via NRF2 to inhibit ferroptosis in lung cancer. *Biochem Pharmacol*. 2025;236:116913. doi:10.1016/j.bcp.2025.116913
26. Chen CT, Wu PH, Hu CC, et al. Aberrant Upregulation of Indoleamine 2,3-Dioxygenase 1 Promotes Proliferation and Metastasis of Hepatocellular Carcinoma Cells via Coordinated Activation of AhR and β-Catenin Signaling. *Int J Mol Sci*. 2021;22(21):1.
27. Zhai L, Ladomersky E, Lenzen A, et al. IDO1 in cancer: a Gemini of immune checkpoints. *Cell Mol Immunol*. 2018;15(5):447–457. doi:10.1038/cmi.2017.143
28. Torres-Martínez L, Morales-Primo AU, Zamora-Chimal J. Indoleamine 2,3-Dioxygenase and Tryptophan Catabolism: key Players in Immunosuppression and Intracellular Parasite Survival Mechanisms. *Immunol Invest*. 2025;1–26. doi:10.1080/08820139.2025.2511079
29. Gao Z, Shao S, Xu Z, et al. IDO1 induced macrophage M1 polarization via ER stress-associated GRP78-XBP1 pathway to promote ulcerative colitis progression. *Front Med Lausanne*. 2025;12:1524952. doi:10.3389/fmed.2025.1524952
30. Zhou Y, Yao L, Ma T, et al. Indoleamine 2,3-dioxygenase-1 involves in CD8(+)T cell exhaustion in glioblastoma via regulating tryptophan levels. *Int Immunopharmacol*. 2024;142(Pt A):113062. doi:10.1016/j.intimp.2024.113062
31. Kenney LL, Chiu RS, Dutra MN, et al. mRNA-delivery of IDO1 suppresses T cell-mediated autoimmunity. *Cell Rep Med*. 2024;5(9):101717. doi:10.1016/j.xcrm.2024.101717
32. de Araújo EF, Feriotti C, Galdino N, et al. The IDO-AhR Axis Controls Th17/Treg Immunity in a Pulmonary Model of Fungal Infection. *Front Immunol*. 2017;8:880. doi:10.3389/fimmu.2017.00880
33. Kai S, Goto S, Tahara K, et al. Indoleamine 2,3-dioxygenase is necessary for cytolytic activity of natural killer cells. *Scand J Immunol*. 2004;59(2):177–182. doi:10.1111/j.0300-9475.2004.01378.x
34. Schmidt SV, Schultze JL. New Insights into IDO Biology in Bacterial and Viral Infections. *Front Immunol*. 2014;5:384. doi:10.3389/fimmu.2014.00384
35. Wang X, Yan B, Li H, et al. Reprogrammed IDO-Induced Immunosuppressive Microenvironment Synergizes with Immunogenic Magnetothermodynamics for Improved Cancer Therapy. *ACS Appl Mater Interfaces*. 2024;16(24):30671–30684. doi:10.1021/acsami.4c02740
36. Yang KD, Zhang X, Shao MC, et al. Aconite aqueous extract inhibits the growth of hepatocellular carcinoma through CCL2-dependent enhancement of natural killer cell infiltration. *J Integr Med*. 2023;21(6):575–583. doi:10.1016/j.joim.2023.10.002
37. Zeng X, Jin X, Leng J, et al. High-dose radiation induces dendritic cells maturation by promoting immunogenic cell death in nasopharyngeal carcinoma. *Front Immunol*. 2025;16:1554018. doi:10.3389/fimmu.2025.1554018
38. Böttcher JP, Reis ESC. The Role of Type 1 Conventional Dendritic Cells in Cancer Immunity. *Trends in Cancer*. 2018;4(11):784–792. doi:10.1016/j.trecan.2018.09.001
39. Jeng LB, Liao LY, Shih FY, et al. Dendritic-Cell-Vaccine-Based Immunotherapy for Hepatocellular Carcinoma: clinical Trials and Recent Preclinical Studies. *Cancers (Basel)*. 2022;14(18):4380. doi:10.3390/cancers14184380
40. Newman AC, Falcone M, Huerta UA, et al. Immune-regulated IDO1-dependent tryptophan metabolism is source of one-carbon units for pancreatic cancer and stellate cells. *Mol Cell*. 2021;81(11):2290–2302. doi:10.1016/j.molcel.2021.03.019
41. Alvarado DM, Chen B, Iticovici M, et al. Epithelial Indoleamine 2,3-Dioxygenase 1 Modulates Aryl Hydrocarbon Receptor and Notch Signaling to Increase Differentiation of Secretory Cells and Alter Mucus-Associated Microbiota. *Gastroenterology*. 2019;157(4):1093–1108. doi:10.1053/j.gastro.2019.07.013
42. Chen B, Alvarado DM, Iticovici M, et al. Interferon-Induced IDO1 Mediates Radiation Resistance and Is a Therapeutic Target in Colorectal Cancer. *Cancer Immunol Res*. 2020;8(4):451–464. doi:10.1158/2326-6066.CIR-19-0282
43. Zheng Q, Gan G, Gao X, et al. Targeting the IDO-BCL2A1-Cytochrome c Pathway Promotes Apoptosis in Oral Squamous Cell Carcinoma. *Onco Targets Ther*. 2021;14:1673–1687. doi:10.2147/OTT.S288692
44. Xing Y, Liu Y, Qi Z, et al. LAGE3 promoted cell proliferation, migration, and invasion and inhibited cell apoptosis of hepatocellular carcinoma by facilitating the JNK and ERK signaling pathway. *Cell Mol Biol Lett*. 2021;26(1):49. doi:10.1186/s11658-021-00295-4
45. Mo C, Xie S, Zhong W, et al. Mutual antagonism between indoleamine 2,3-dioxygenase 1 and nuclear factor E2-related factor 2 regulates the maturation status of DCs in liver fibrosis. *Free Radic Biol Med*. 2020;160:178–190. doi:10.1016/j.freeradbiomed.2020.07.038
46. Kimura T, Romera L, de Almeida SR. Fonsecaea pedrosoi Conidia Induces Activation of Dendritic Cells and Increases CD11c(+) Cells in Regional Lymph Nodes During Experimental Chromoblastomycosis. *Mycopathologia*. 2020;185(2):245–256. doi:10.1007/s11046-020-00429-w
47. Mo C, Xie S, Zeng T, et al. Ginsenoside-Rg1 acts as an IDO1 inhibitor, protects against liver fibrosis via alleviating IDO1-mediated the inhibition of DCs maturation. *Phytomedicine*. 2021;84:153524. doi:10.1016/j.phymed.2021.153524
48. Hammer A, Waschbisch A, Knippertz I, et al. Role of Nuclear Factor (Erythroid-Derived 2)-Like 2 Signaling for Effects of Fumaric Acid Esters on Dendritic Cells. *Front Immunol*. 2017;8:1922. doi:10.3389/fimmu.2017.01922
49. Ma S, Yang J, Li J, et al. The clinical utility of the proliferating cell nuclear antigen expression in patients with hepatocellular carcinoma. *Tumour Biol*. 2016;37(6):7405–7412. doi:10.1007/s13277-015-4582-9
50. Yang P, Zhang J. Indoleamine 2,3-Dioxygenase (IDO) Activity: a Perspective Biomarker for Laboratory Determination in Tumor Immunotherapy. *Biomedicines*. 2023;11(7):1988. doi:10.3390/biomedicines11071988
51. Glamočlija S, Sabljić L, Tomić S, et al. Trichinella spiralis extracellular vesicles induce anti-inflammatory and regulatory immune responses in vitro. *Int J Parasitol*. 2025;55(6):299–315. doi:10.1016/j.ijpara.2025.01.008
52. Vogel CF, Wu D, Goth SR, et al. Aryl hydrocarbon receptor signaling regulates NF-κB RelB activation during dendritic-cell differentiation. *Immunol Cell Biol*. 2013;91(9):568–575. doi:10.1038/icb.2013.43
53. Zhu L, Shang J, Li Y, et al. Toll-Like Receptors Mediate Opposing Dendritic Cell Effects on Treg/Th17 Balance in Mice With Intracerebral Hemorrhage. *Stroke*. 2024;55(8):2126–2138. doi:10.1161/STROKEAHA.124.046394
54. Albini E, Rosini V, Gargaro M, et al. Distinct roles of immunoreceptor tyrosine-based motifs in immunosuppressive indoleamine 2,3-dioxygenase 1. *J Cell Mol Med*. 2017;21(1):165–176. doi:10.1111/jcmm.12954

55. Asgari F, Nikzamir A, Baghaei K, et al. Immunomodulatory and Anti-Inflammatory Effects of Vitamin A and Tryptophan on Monocyte-Derived Dendritic Cells Stimulated with Gliadin in Celiac Disease Patients. *Inflammation*. 2024;47(5):1706–1727. doi:10.1007/s10753-024-02004-7
56. Panfili E, Mondanelli G, Orabona C, et al. The catalytic inhibitor epacadostat can affect the non-enzymatic function of IDO1. *Front Immunol*. 2023;14:1134551. doi:10.3389/fimmu.2023.1134551
57. Liu W, Zhou H, Lai W, et al. Artesunate induces melanoma cell ferroptosis and augments antitumor immunity through targeting Ido1. *Cell Commun Signal*. 2024;22(1):378. doi:10.1186/s12964-024-01759-8
58. Chen L, Cheng S, Ying J, et al. Aristolochic acid I promotes renal tubulointerstitial fibrosis by up-regulating expression of indoleamine 2,3-dioxygenase-1 (IDO1). *Toxicol Lett*. 2024;402:44–55. doi:10.1016/j.toxlet.2024.11.003
59. Guangzhao L, Xin W, Miaoqing W, et al. IDO1 inhibitor enhances the effectiveness of PD-1 blockade in microsatellite stable colorectal cancer by promoting macrophage pro-inflammatory phenotype polarization. *Cancer Immunol Immunother*. 2025;74(2):71. doi:10.1007/s00262-024-03925-w
60. Wang Y, Wu Y, Jiang H, et al. L-Kynurenine activates the AHR-PCSK9 pathway to mediate the lipid metabolic and ovarian dysfunction in polycystic ovary syndrome. *Metabolism*. 2025;168:156238. doi:10.1016/j.metabol.2025.156238
61. Tahaghoghi-Hajghorbani S, Yazdani M, Nikpoor AR, et al. Targeting the tumor microenvironment by liposomal Epacadostat in combination with liposomal gp100 vaccine. *Sci Rep*. 2023;13(1):5802. doi:10.1038/s41598-023-31007-x
62. Bilir C, Eskiler GG, Bilir F. The cytotoxic effects of indoleamine 2, 3-dioxygenase inhibitors on triple negative breast cancer cells upon tumor necrosis factor α stimulation. *J Cancer Res Ther*. 2023;19(Supplement):S74–S80. doi:10.4103/jcrt.jcrt_2365_21
63. Long GV, Dummer R, Hamid O, et al. Epacadostat plus pembrolizumab versus placebo plus pembrolizumab in patients with unresectable or metastatic melanoma (ECHO-301/KEYNOTE-252): a Phase 3, randomised, double-blind study. *Lancet Oncol*. 2019;20(8):1083–1097. doi:10.1016/S1470-2045(19)30274-8
64. Sheykhhasan M, Ahmadieh-Yazdi A, Heidari R, et al. Revolutionizing cancer treatment: the power of dendritic cell-based vaccines in immunotherapy. *Biomed Pharmacother*. 2025;184:117858. doi:10.1016/j.biopha.2025.117858
65. Bol KF, Schreibelt G, Bloemendal M, et al. Adjuvant dendritic cell therapy in stage IIIB/C melanoma: the MIND-DC randomized phase III trial. *Nat Commun*. 2024;15(1):1632. doi:10.1038/s41467-024-45358-0
66. Van TLF, Willemsen M, Bezemer K, et al. Dendritic Cell-Based Immunotherapy in Patients With Resected Pancreatic Cancer. *J Clin Oncol*. 2024;42(26):3083–3093. doi:10.1200/JCO.23.02585
67. Hunig T. T-cell function and specificity in athymic mice. *Immunol Today*. 1983;4(3):84–87. doi:10.1016/0167-5699(83)90125-1
68. Raff MC. Theta-bearing lymphocytes in nude mice. *Nature*. 1973;246(5432):350–351. doi:10.1038/246350a0
69. MacDonald HR, Lees RK, Sordat B, et al. Age-associated increase in expression of the T cell surface markers Thy-1, Lyt-1, and Lyt-2 in congenitally athymic (nu/nu) mice: analysis by flow microfluorometry. *J Immunol*. 1981;126(3):865–870. doi:10.4049/jimmunol.126.3.865
70. Schedi MP, Goldstein G, Boyce EA. Differentiation of T cells in nude mice. *Science*. 1975;190(4220):1211–1213. doi:10.1126/science.190.4220.1211
71. Dennert G, Hyman R. Functional Thy-1+ cells in cultures of spleen cells from nu/nu mice. *Eur J Immunol*. 1980;10(8):583–589. doi:10.1002/eji.1830100803
72. Gillis S, Union NA, Baker PE, et al. The in vitro generation and sustained culture of nude mouse cytolytic T-lymphocytes. *J Exp Med*. 1979;149(6):1460–1476. doi:10.1084/jem.149.6.1460
73. Hünig T, Bevan MJ. Specificity of cytotoxic T cells from athymic mice. *J Exp Med*. 1980;152(3):688–702. doi:10.1084/jem.152.3.688
74. MacDonald HR, Lees RK. Frequency and specificity of precursors of interleukin 2-producing cells in nude mice. *J Immunol*. 1984;132(2):605–610. doi:10.4049/jimmunol.132.2.605
75. Neu F, Rebai T, Denef JF, et al. Involvement of T cell immunity in the transient thyroid inflammation induced by iodide in goitrous BALB/C and nude mice. *Autoimmunity*. 1994;17(3):209–216. doi:10.3109/08916939409010656
76. Kim HE, Na YG, Jin M, et al. Fabrication and evaluation of chitosan-coated nanostructured lipid carriers for co-delivery of paclitaxel and PD-L1 siRNA. *Int J Pharm*. 2024;666:124835. doi:10.1016/j.ijpharm.2024.124835
77. Run ZZ, Ma K, Yue LH, et al. High-fat diet alters immune cells in spleen, kidney and tumor and impacts the volume growth of renal cell carcinoma. *Int Immunopharmacol*. 2023;124(Pt B):110982. doi:10.1016/j.intimp.2023.110982
78. Deng Z, Teng YJ, Zhou Q, et al. Shuyu pills inhibit immune escape and enhance chemosensitization in hepatocellular carcinoma. *World J Gastrointest Oncol*. 2021;13(11):1725–1740. doi:10.4251/wjgo.v13.i11.1725